AJNR

Fast Detection of Diffuse Axonal Damage in Severe Traumatic Brain Injury: Comparison of Gradient-Recalled Echo and Turbo Proton Echo-Planar Spectroscopic Imaging MRI Sequences

Elisabetta Giugni, Umberto Sabatini, Gisela E. Hagberg, Rita Formisano and Alessandro Castriota-Scanderbeg

AJNR Am J Neuroradiol 2005, 26 (5) 1140-1148
http://www.ajnr.org/content/26/5/1140

Fast Detection of Diffuse Axonal Damage in Severe Traumatic Brain Injury: Comparison of Gradient-Recalled Echo and Turbo Proton Echo-Planar Spectroscopic Imaging MRI Sequences

Elisabetta Giugni, Umberto Sabatini, Gisela E. Hagberg,
Rita Formisano, and Alessandro Castriota-Scanderbeg

BACKGROUND AND PURPOSE: **Diffuse axonal injury (DAI) is a common type of primary neuronal injury in patients with severe traumatic brain injury (TBI), and is frequently accompanied by tissue tear hemorrhage. T2*-weighted gradient-recalled echo (GRE) sequences are more sensitive than T2-weighted spin-echo images for detection of hemorrhage. The purpose of this study is to compare turbo Proton Echo Planar Spectroscopic Imaging (t-PEPSI), an extremely fast sequence, with GRE sequence in the detection of DAI.**

METHODS: **Twenty-one patients (mean age 26.8 years) with severe TBI occurred at least 3 months earlier, underwent a brain MR Imaging study on a 1.5-T scanner. A qualitative evaluation of the t-PEPSI sequences was performed by identifying the optimal echo time and in-plane resolution. The number and size of DAI lesions, as well as the signal intensity contrast ratio (SI CR), were computed for each set of GRE and t-PEPSI images, and divided according to their anatomic location as lobar and/or deep brain.**

RESULTS: **There was no significant difference between GRE and t-PEPSI sequences in the detection of the total number of DAI lesions (291 vs. 230, respectively). GRE sequence delineated a higher number of DAI in the temporal lobe compared to the t-PEPSI sequence (74 vs. 37, $P < .004$), while no differences were found for the other regions. The SI CR was significantly lower with the t-PEPSI than the GRE sequence ($P < .00001$).**

CONCLUSION: **Owing to its very short scan time and high sensitivity to the hemorrhage foci, the t-PEPSI sequence may be used as an alternative to the GRE to assess brain DAI in severe TBI patients, especially if uncooperative and medically unstable.**

Diffuse axonal injury (DAI) is one of the most common types of primary neuronal injury in patients with severe traumatic brain injury (TBI). DAI without massive brain damage is estimated to occur in almost 50% of patients with a severe head injury, and it is the most common cause of vegetative states and severe disability after TBI (1, 2). DAI is a widespread disruption of axons that occurs during abrupt acceleration or deceleration. The crucial factors to the extent of injury are the type of acceleration and deceleration (angular rather than translational), the duration of acceleration and deceleration (long rather than short), and the direction of head movement (coronal rather than sagittal) (3).

Received June 24, 2004; accepted after revision October 6.

From the IRCCS, Fondazione S. Lucia, Rome, Italy.

Address reprint requests to Elisabetta Giugni, MD, IRCCS, Fondazione S. Lucia Via Ardeatina 306 Rome 00179 Italy.

Radiologic recognition of DAI can be of the utmost importance to understanding the clinical syndrome and predicting the patient's outcome. Unfortunately, DAI is frequently underestimated on CT and conventional MR imaging (4–7).

DAI lesions tend to be multiple and small. Common sites are the corpus callosum, the gray matter–white matter junction in parasagittal areas, the deep periventricular white matter (especially in the frontal area at the corner of the ventricles), the basal ganglia and internal capsule, the hippocampal and parahippocampal regions, the dorsolateral aspect of the brainstem, and the cerebellum (4, 8, 9).

The MR imaging appearance of DAI lesions depends on several factors, including the time since injury, the presence of hemorrhage or blood-breakdown products, and the type of sequence used. In the acute and early subacute phases, susceptibility effects largely occur from deoxyhemoglobin and methemoglobin forms of hemoglobin. The T2*-weighted gra-

dient-recalled echo (GRE) sequence has been reported to be more sensitive than T2-weighted spin-echo (SE) sequence to the magnetic susceptibility induced by static field inhomogeneities, arising from paramagnetic blood breakdown products (6, 10, 11). T2-weighted SE and fluid-attenuated inversion recovery (FLAIR) MR imaging sequences nicely depict small, nonhemorrhagic shearing injuries as hyperintense lesions. Because of their sensitivity to susceptibility changes, GRE MR images permit the identification of most blood products, such as deoxyhemoglobin, methemoglobin, and hemosiderin, which are all paramagnetic substances in the white matter (12). Moreover, Fazekas et al (13) provided histopathologic support for the concept that focal areas of signal intensity (SI) loss on T2*-weighted MR images correspond to hemosiderin deposits in the absence of other possibly related morphologic abnormalities, such as focal calcifications or small vascular malformations. These foci of blood products, caused by disruption of penetrating blood vessels, are often undetected on conventional T1- and T2-weighted images alone (14, 15).

If we consider that T1- and T2-weighted imaging is necessary to obtain morphologic details of the lesions and that GRE images improve the detection of hemorrhagic lesions that occur in 10–30% of patients with DAI (15), the use of ultrafast sequences sensitive to inhomogeneities of the static magnetic field is desirable to minimize the examination time.

Echo-planar imaging (EPI) is an ultrafast MR imaging technique that uses a train of oscillating frequency-encoding gradients to traverse k-space, enabling the rapid acquisition of data. It has a number of clinical applications, including perfusion and diffusion imaging of acute ischemic stroke, and functional imaging. Furthermore, the speed of EPI minimizes motion artifacts and could improve the evaluation of patients with trauma, especially if they are uncooperative, medically unstable, pediatric, or claustrophobic (16, 17). However, EPI has some disadvantages compared with conventional T2*-weighted (e.g., GRE) techniques, including increased geometric distortions and magnetic susceptibility artifacts. To limit the effect of such drawbacks, EPI with a small voxel can be used.

The spectroscopic imaging method called proton echo-planar spectroscopic imaging (PEPSI) (18) has been developed into a new multi-EPI sequence that is sensitive to static magnetic field inhomogeneities. The turbo-PEPSI (t-PEPSI) technique has been used to increase the sensitivity of functional MR imaging (19) and to permit the absolute quantification of T2* and proton density values (20). This method provides several-echo images in a single shot at a speed comparable to that of conventional EPI, and it is sensitive to static magnetic field inhomogeneities.

Compared with conventional EPI sequences, the t-PEPSI sequence gives more information (i.e., measurement of T2* weighting at several TEs) without prolonging the examination time. To date, few have compared the sensitivity of GRE and EPI sequences in detecting foci of intracranial hemorrhage (21–23), and to our knowledge, no groups have studied DAI lesions associated with severe TBI by using t-PEPSI. Therefore, we used this technique to determine the optimal EPI measurement protocol to detect lesions with susceptibility changes in DAI. The aims of this study were to compare the GRE and t-PEPSI sequences in their ability to detect susceptibility dephasing caused by the deposition of blood products associated with DAI and to determine whether the t-PEPSI sequence can be used as an alternative to the GRE sequence to assess DAI in patients with severe TBI.

TABLE 1: Demographic and clinical data of 21 patients with severe TBI

Patient/ Sex/Age (y)	Coma Duration (d)	Interval, TBI to MR Imaging (mo)	Glasgow Outcome Scale Score
1/M/23	30	3	5
2/M/20	18	8	4
3/M/18	25	6	4
4/F/21	7	3	5
5/F/37	18	26	5
6/M/25	30	4	5
7/M/26	21	30	4
8/M/30	10	73	5
9/M/20	26	13	3
10/M/31	30	18	4
11/M/26	27	4	4
12/M/20	5	29	4
13/M/28	15	9	4
14/M/22	15	3	5
15/M/38	15	3	4
16/M/31	30	112	4
17/M/18	21	25	3
18/M/35	40	16	3
19/M/30	15	6	4
20/M/40	80	154	4
21/M/24	20	17	3

Methods

Patients

We prospectively obtained and compared GRE and t-PEPSI images in 21 patients with severe TBI and suspected DAI (19 men, two women; age range 18–40 years; mean age, 26.8 years). Table 1 shows their demographic and clinical data. All patients underwent brain MR imaging at least 3 months after trauma. By the time of their MR examination, all patients had been clinically assessed using the Glasgow Outcome Scale (24). Inclusion criteria were the diagnosis of severe brain injury according to the Glasgow Coma Scale score (25) and a history of coma longer than 48 hours. Patients with neurosurgical sequelae and those with posttraumatic hydrocephalus were excluded.

MR Imaging

In all patients, a 1.5-T system (Vision; Siemens Medical Systems, Erlangen, Germany) with EPI capabilities was used for the MR examinations. The imaging protocol was the following: (1) conventional SE T1-weighted images (TR/TE/NEX = 650/14/2, flip angle = 70°, bandwidth per pixel = 89 Hz, matrix = 256 × 256, in-plane resolution = 0.9 × 0.9 mm,

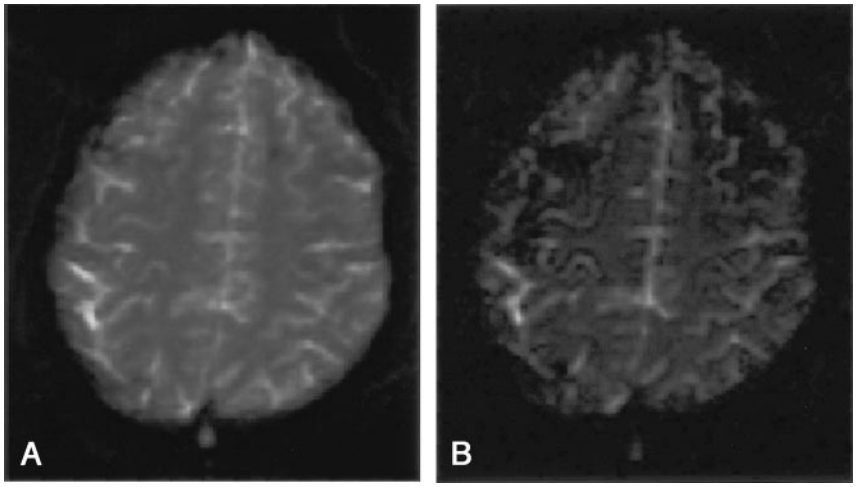

FIG 1. Dual-echo high resolution t-PEPSI sequence (TR/TE1/TE2/NEX = 5000/50/145/1, flip angle = 90°).

A, First-echo image obtained shows good lesion-to-tissue contrast.

B, Second image in the same shot is not of satisfactory quality for lesion detection.

and acquisition time = 4 minutes 10 seconds), (2) double-echo turbo SE proton density–and T2-weighted images (TR/TE1/TE2/NEX = 3800/22/90/1, bandwidth per pixel = 130 Hz, matrix = 256 × 256, in-plane resolution = 0.9 × 0.9 mm, and acquisition time = 2 minutes 15 seconds), (3) GRE fast low-angle shot (FLASH, TR/TE/NEX = 777/15/2, flip angle = 15°, bandwidth per pixel = 78 Hz, matrix = 256 × 256, in-plane resolution = 1.0 × 1.0 mm, and acquisition time 4 minutes 15 seconds), and (4) dual-echo t-PEPSI, (TR/TE1/TE2/NEX = 5000/50/145/1, flip angle = 90°, bandwidth per pixel = 1190 Hz, matrix = 96 × 128, in-plane resolution = 1.7 × 1.7 mm, and acquisition time = 5 seconds).

In a subgroup of five patients, we also used a four-echo t-PEPSI protocol (TR/TE1/TE2/TE3/TE4/NEX = 5000/23/64/105/145/1, flip angle = 90°, bandwidth per pixel = 2080 Hz, matrix = 64 × 64, in-plane resolution = 3 × 3 mm, and acquisition time = 5 seconds).

For each sequence, 20 5-mm-thick axial sections with a 1-mm intersection gap were positioned to run parallel to the anterior commissure–posterior commissure line and co-localized.

Image Analysis

Unlike conventional EPI sequences, t-PEPSI allows for measurement of the degree of T2* weighting at several TEs in a single shot, without requiring extra time for the examination. We used two versions of the t-PEPSI sequence, each with a different voxel size and TE to determine the best imaging parameters for the detection of DAI lesions. We compared the sequences to establish which was best for detecting DAI lesions.

DAI were defined as areas of abnormally low signal intensity (SI) on GRE and t-PEPSI images. Two experienced neuroradiologists (A.C.-S., U.S.), who were unaware of the patient's identity, independently reviewed all images on a computer display in a random mode. Areas of abnormal hypointensity were identified on both sequences by consensus. The images could not be graded in a blinded fashion because inherent SI characteristics and unique artifacts always differentiated the two sequences. After the lesions were identified, a third operator (E.G.) manually drew regions of interest (ROIs). ROIs were classified according to their anatomic location, as lobar (frontal, temporal, parietal, occipital) and/or deep brain regions (basal ganglia, periventricular, corpus callosum and infratentorial). The diameter and area for each ROI were recorded, and the total number of ROIs was calculated. Images acquired with the two sequences were reviewed side by side to determine the number and size of shared lesions shown on both and the number of DAI lesions seen with either sequence alone.

SI in the lesions and in symmetric areas of the normal parenchyma in the contralateral hemisphere were analyzed. The signal-to-contrast ratio (CR) was measured according to the following equation: $SI\ CR = (SI_{lesion} - SI_{contralateral\ normal\ parenchyma})/SI_{contralateral\ normal\ parenchyma}$. All image analyses were performed by using software (MEDx, version 3.0; Sensor Systems, Inc., Sterling, VA) running on a workstation (UNIX Octane, Silicon Graphics, Inc., Mountain View, CA).

Statistical Analysis

A Wilcoxon signed rank test was used to compare the number of hypointense lesions detected by using the GRE sequence and the number detected by using the t-PEPSI sequence. Analysis of variance was also performed to determine significant differences in CR between the two sequences. The level of statistical significance was set at 1% ($P < .01$).

Results

The ability of t-PEPSI to depict DAI lesions was strongly dependent on the selected sequence and, hence, the imaging parameters. As Figure 1 shows, the first echo of the dual-echo high-resolution t-PEPSI sequence with a TE of 50 msec showed excellent lesion-to-tissue contrast (Fig 1A), whereas the second image in the same shot with a TE of 145 msec was unsatisfactory for lesion detection (Fig 1B). In the subgroup of five patients examined by using the four-echo t-PEPSI sequence, lesion susceptibility could not be elicited at a TE of 23 msec corresponding to the first echo image of the sequence (Fig 2A). The best lesion-to-tissue contrast was again obtained at a TE of around 50 msec (Fig 2B), whereas with a longer TE of 100 or 145 msec (Fig 2C and D), lesion-to-tissue contrast decreased substantially. We observed heavy susceptibility artifacts at the air-tissue interface, and hence lower sensitivity, for the four-echo t-PEPSI sequences compared with the dual-echo t-PEPSI sequence.

On the basis of these results, further analysis was carried out by using only the first echo of the high-resolution dual-echo t-PEPSI sequence. Table 2 summarizes the results. We counted 371 DAI in 21 patients with severe TBI by using the GRE and t-PEPSI sequences. GRE images depicted more total hypointense lesions than the t-PEPSI sequence (291 vs. 230),

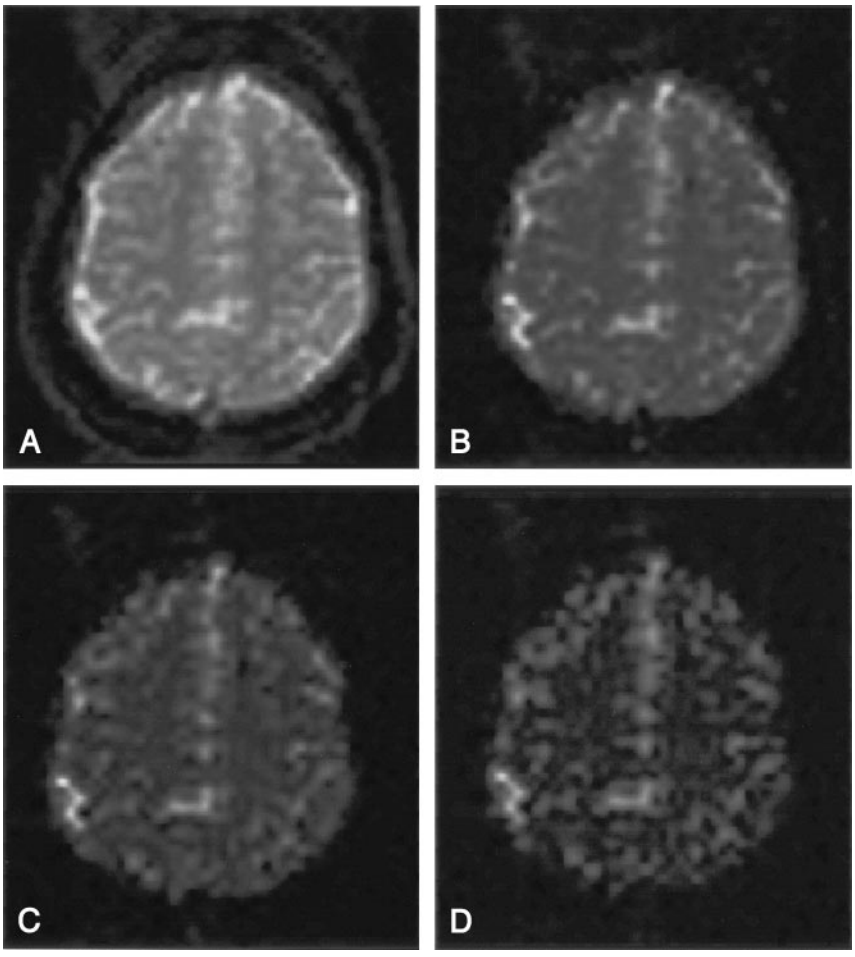

FIG 2. Four-echo t-PEPSI images (TR/TE1/TE2/TE3/TE4/NEX = 5000/23/64/105/145/1, flip angle = 90°).

A, On the first-echo image, susceptibility effects of the lesion have not affected the image contrast to a great extent.

B, Best lesion-to-tissue contrast is obtained around 50 msec.

C and *D*, At longer TEs, contrast is lost.

TABLE 2: DAI lesions detected with the two sequences in 21 patients with severe TBI

Location of Lesion	Lesions Detected			
	GRE Imaging	t-PEPSI	Only on GRE Imaging	Only on t-PEPSI
Whole brain (n = 371)	291	230	141	80
Frontal lobe (n = 158)	126	98	60	32
Temporal lobe (n = 88)	74*	37*	51	14
Parietal lobe (n = 30)	22	20	10	8
Occipital lobe (n = 9)	7	8	1	2
Basal ganglia (n = 28)	23	20	8	5
Corpus callosum (n = 22)	12	18	4	10
Periventricular (n = 13)	10	12	1	3
Infratentorial (n = 23)	17	17	6	6

* P <.004, Wilcoxon test.

TABLE 3: Characteristics of 150 small DAI lesions detected on GRE and t-PEPSI images

Small Lesions*	GRE Sequence	t-PEPSI Sequence
No.	130 (86.7)	87 (58.0)
Mean diameter (mm)	3.46 ± 2.07	4.92 ± 3.12
Mean area (mm^2)	12.74 ± 21.73	26.56 ± 39.18

Note.—Data are the number or the mean ± standard deviation. Data in parentheses are percentages.

* Diameter ≤5 mm.

but the difference was not significant (P = .07). The consensus side-by-side review revealed that, in the whole brain, 150 DAI lesions were visible on images obtained with both sequences, 141 lesions were identified on only GRE images, and 80 were depicted on only t-PEPSI images. Moreover, the GRE sequence was superior to the t-PEPSI sequence in depicting DAI lesions in the temporal lobe (74 vs. 37, P < .004). In the remaining cerebral regions, both sequences had similar sensitivities in lesion detection, without any significant difference.

Among the 150 DAI lesions shown with both sequences, 130 (86.7%) small lesions (diameter ≤5.0 mm) were detected by using the GRE sequence, and 87 (58%) by using the t-PEPSI sequence (Table 3). This result suggested that DAI lesions identified on t-PEPSI images were larger than those on GRE images because of the stronger susceptibility effect of hemorrhagic foci associated with the t-PEPSI sequence.

Last, among DAI lesions shown with both sequences, SI CR was significantly lower with the t-PEPSI than the GRE sequence (−0.39 ± 0.17 vs. −0.26 ± 0.14, P < .00001), resulting in improved lesion conspicuity. For both sequences, SI CR was

independent of lesion size, as this value did not differ among lesions of different sizes ($P = .07$).

Discussion

Results of experimental studies of TBI suggest that diffuse neuronal damage and cell loss may progress over weeks to months after the initial insult and that various MR imaging techniques applied at early and delayed times can provide useful information about the severity of injury and the clinical outcomes (26–32).

CT scans and conventional MR images provide poor predictors of functional outcome in patients with TBI. Specifically, DAI is frequently underestimated by using these imaging modalities (4–7). Although results of one study suggests otherwise (6), the correct assessment of DAI seems important in terms of short- and long-term outcomes and in planning proper rehabilitation. In addition, some patients with TBI may benefit from early treatment with amantadine (during the first 3 months after TBI), whereas others with damage to the substantia nigra and tegmentum may respond to dopaminergic drug agonists (33–36).

Data from the literature suggest that GRE sequences are particularly suited to depict DAI lesions (15). Because of their sensitivity to susceptibility effects, GRE sequences are recommended in patients with TBI, in combination with conventional MR imaging (T1-weighted SE, T2-weighted SE, and FLAIR imaging) to improve the detection of hemorrhagic DAI lesions (15). Most blood products, such as deoxyhemoglobin, methemoglobin, and hemosiderin, are often undetected on conventional MR images alone. On the other hand, these images are necessary because of their ability to depict areas of gliosis or tissue necrosis, which are often associated with brain trauma, and to provide detailed anatomic information about brain lesions. Iron deposits can be detected with T2*-weighted sequences, and the GRE technique is most commonly used. GRE sequences can be optimized to reduce the acquisition time to less than 2 minutes, but their relatively long acquisition times is a drawback when they are performed in addition to routine clinical imaging. This may be a serious limitation in some patients, especially if they are uncooperative, claustrophobic, or medically unstable. Our results suggest that t-PEPSI can be used as an alternative to the GRE sequence, given the reduction in both acquisition time (seconds vs. minutes) and motion artifacts.

The EPI sequence is the fastest MR imaging technique currently available, owing to its efficient sampling scheme that allows coverage of the whole brain in as little as 3–5 seconds, depending on gradient hardware. Limitations of EPI are geometric distortion, increased magnetic susceptibility effects, intrinsic T2* effects resulting in a loss of resolution, and chemical-shift artifacts that require fat suppression (37, 38). Geometric distortions and susceptibility effects can be mitigated by using fast image acquisition, which can be achieved by increasing the sampling rate, limiting the matrix size in the read-out direction, and other means. Furthermore, TE affects image artifacts, where a short TE reduces susceptibility effects at the tissue-air boundaries. On the contrary, high resolution and optimal TE (for maximizing lesion-to-tissue contrast) are required to detect DAI lesions.

We set out to optimize the EPI measurement protocol for the detection of lesions with susceptibility changes in DAI. We therefore used two t-PEPSI sequences: one with few echoes and high resolution and another with several echoes and lower resolution. This approach enabled a direct comparison of images obtained at different TEs with different voxel sizes. Specifically, we found that EPI with a TE of around 50 msec and a pixel small than 2×2 mm gave the best results in terms of lesion contrast and restricted susceptibility artifacts at tissue-air boundaries. On T2*-weighted images, available SI decays with the effective transverse relaxation time, which in turn depends on two parameters: the microscopic T2 relaxation and an additional dephasing, T2′, caused by inhomogeneities in the local static magnetic field, like those arising in and around hemorrhagic lesions. To image small lesions in TBI, the lesion is generally smaller than the voxel, and the T2′ dephasing manifests as a constant additional contribution to the local T2 SI decay. In practice, lesion contrast increases with TE up to values given by the actual T2* values in tissue with lesions and that without lesions. Beyond this limit, contrast decreases until no appreciable contrast between the two tissue types can be detected.

At 1.5 T, the optimal TE for lesion detection seemed to be around 50 msec, in agreement with previous reports (39), regardless of voxel size. Nevertheless, it may be desirable to increase the in-plane resolution with the t-PEPSI sequence even further to investigate whether additional lesion conspicuity can be gained. However, exceeding the resolution applied in the present study may bring about some potential difficulties: The time needed for the single-shot read-out would increase considerably, and hence, the bandwidth would decrease. The SI-to-noise ratio would also increase, but so would geometric distortion and susceptibility artifacts, which are undesirable for detection of lesions near air-tissue interfaces. Moreover, to achieve a 256×256 resolution with a single-shot EPI sequence and TEs around 50 msec, the rate of gradient switching would have to increase, and the limit for cardiac nerve stimulation could potentially be exceeded. Therefore, in practice, EPI with such high in-plane resolutions cannot be performed on whole-body systems, but they may be considered in future studies on head-only dedicated MR machines.

Our results suggest that the GRE and t-PEPSI sequences are equivalent in identifying the total number of DAI lesions, except for lesions in the temporal lobes, where the GRE sequence was superior. In comparison, DAI lesions that were detected on both types of images appeared to be larger and to have a lower SI CR ratio (darker appearance), regardless of lesion size, on t-PEPSI than on GRE imaging. The result was more straightforward detection of the lesions when t-PEPSI was used.

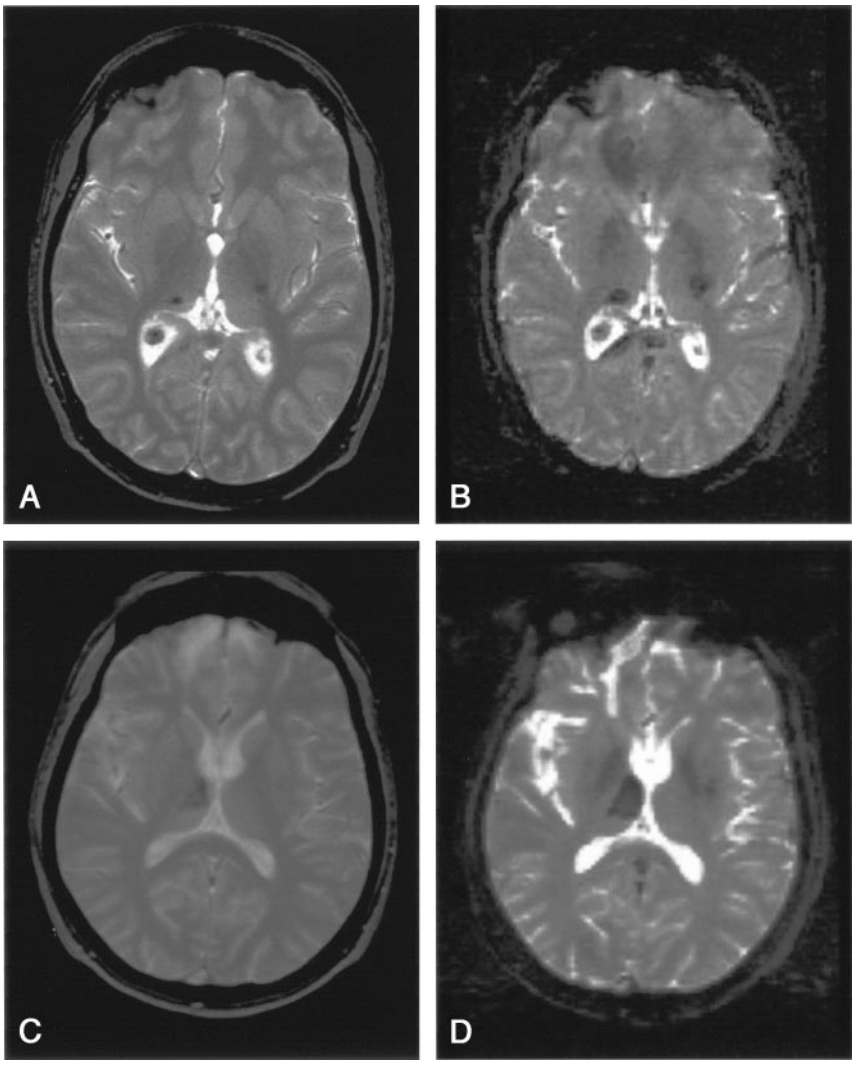

FIG 3. Location of DAI lesions in deep intra-axial structures.

A and *B*, GRE (*A*) and t-PEPSI (*B*) images show lesions in the corpus callosum, posterior left internal capsule, and right thalamus.

C and *D*, GRE (*C*) and t-PEPSI (*B*) images show a right thalamic lesion.

Only a few groups have investigated the role of the EPI sequences for the assessment of structural brain lesions, and, to our knowledge, none have studied the use of an ultrafast sequence to detect DAI lesions in patients with severe TBI (11, 21, 22). In previous studies, GRE-type single-shot EPI was compared with conventional GRE FLASH imaging to assess their relative ability to depict chronic hemorrhagic foci in patients with brain tumor, arteriovenous malformation, cavernous angioma, chronic hematoma, neurosyphilis, or brain contusion (in a single patient) (21). This study showed that GRE EPI sequences are comparable to FLASH sequences for the detection of supratentorial hemorrhagic areas but inferior for the detection of infratentorial lesions. More recently, Tong et al (12) compared the effectiveness of a high-spatial-resolution, susceptibility-weighted MR imaging technique with conventional GRE MR imaging for the detection of hemorrhage in children and adolescents with DAI. Susceptibility-weighted MR imaging depicted much smaller hemorrhagic lesions than GRE imaging. This work was based on postprocessed images obtained from combined phase and magnitude imaging, which has also proved useful for the detection of occult vascular lesions (40). Although these reports give evidence of impressive image quality, their technique may be hampered in clinical practice, requires fast image acquisition in uncooperative patients, as the current acquisition times for susceptibility-weighted MR imaging are on the order of 10 minutes.

Unlike the previous findings, we found no significant difference between the GRE and t-PEPSI sequences in their ability to depict DAI lesions in 21 patients with severe TBI. In fact, both sequences depicted a similar total number of hypointense lesions scattered throughout the whole brain, without regional-dependent differences, except for the temporal lobes, where the t-PEPSI sequence depicted about 50% of the DAI lesions found with the GRE technique. The lower sensitivity of the t-PEPSI was most likely due to the geometric distortion and magnetic susceptibility artifacts at the tissue-air boundaries. Altogether, our results suggest that image distortion is not a major problem in the evaluation of infratentorial DAI lesions. Of note, we optimized the parameters of the t-PEPSI sequence to minimize image imperfections: The sampling rate was decreased

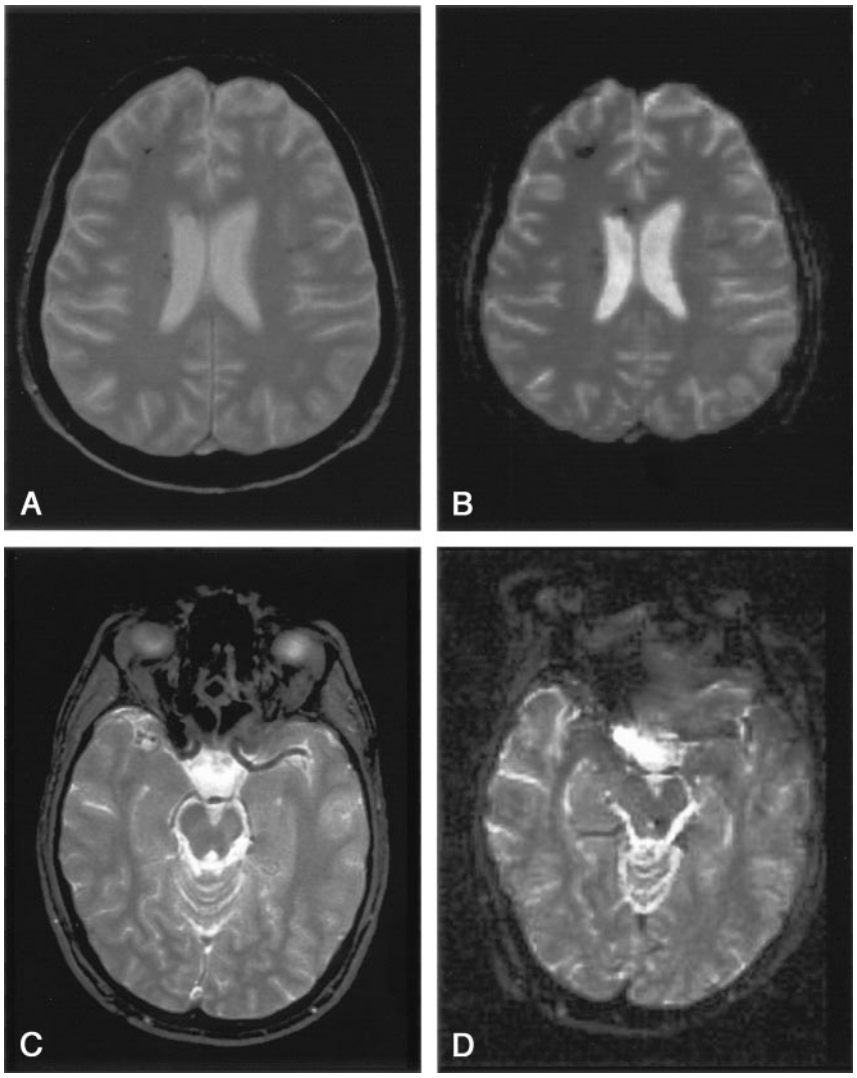

FIG 4. Location of DAI lesions in the deep intra-axial structures.

A and *B*, Lesions in the periventricular white matter and corpus callosum on GRE (*A*) and t-PEPSI (*B*) images.

C and *D*, GRE image (*C*) shows slightly abnormal decrease in SI in the left mesial temporal region and in the left posterior lateral of the midbrain. Both lesions are more easily identified on the t-PEPSI image (*D*).

to 1160 Hz per pixel and 96 instead of 128 read-out trains were acquired with the dual echo t-PEPSI acquisition.

Nevertheless, other factors may explain the discrepancy between our results and previously published data (21). DAI lesions are a special category of brain injury that most frequently involves the brainstem and structures in the deep white matter (41). The severity and localization of shearing injury are initially determined by mainly the direction and magnitude of the rotational acceleration or deceleration forces and by the difference in attenuation and rigidity between two adjacent tissues (e.g., cerebral gray matter and white matter) (9). The anatomy of the skull base explains the specific vulnerability of the adjacent cerebral tissue to rotational forces. With t-PEPSI sequences, the centroaxial structures appear to be free from geometric distortion and susceptibility effects at the tissue-air boundaries, resulting in an equal ability of both sequences to depict DAI lesions. Similarly, our data showed that t-PEPSI sequences were comparable to GRE sequences in the detection of hemorrhagic lesions in the deep structures, notably the corpus callosum (18 and 12, respectively), periventricular area (12 vs. 10), and basal ganglia (23 vs. 20) (Fig 3, 4). The ability of t-PEPSI to depict injury to the corpus callosum is of utmost importance because damage in this area indicates a shearing force of sufficient degree to produce widespread DAI. Data from the literature show that a combination of lesions in the corpus callosum and the dorsolateral upper brainstem is a frequent MR imaging feature in patients in posttraumatic vegetative states associated with DAI. Injury to the corpus callosum is an indicator of other possible midline lesions, particularly in the brainstem, which may be responsible for unconsciousness (32, 42, 43).

Concerning the size of DAI lesions shown with both sequences, our results indicate that the increased size of lesions on t-PEPSI was probably due to increased sensitivity to susceptibility effects with this sequence, and the resulting blooming effect of lesions with susceptibility changes could improve the sensitivity of this sequence in case of small DAI lesions that may go undetected with conventional GRE sequences. A further finding of was the significantly decreased SI CR of lesions on t-PEPSI compared with GRE imaging; this resulted in improved detec-

tion of the DAI lesions even when patients could not hold a given position for a prolonged time (seconds vs. minutes). In other words: the EPI-based sequence improved lesion conspicuity compared with conventional methods, despite the short acquisition time. An additional improvement that may be considered in future studies is increasing the number of excitations, followed by averaging: Indeed, five t-PEPSI acquisitions within a 20-second acquisition time would be acceptable in most patients with TBI.

Altogether, our results suggest that an optimized t-PEPSI sequence, though it is less sensitive than a conventional GRE sequence, may be used as an alternative technique for identifying DAI lesions in unstable or uncooperative patients with severe TBI.

Conclusion

Substantial benefits may be gained from rapid T2*-weighted MR imaging in patients with severe TBI. Patient throughput may be increased, image degradation from gross motion artifacts may be diminished, and sensitivity for small DAI lesions (which would be otherwise undetected) can be increased. Although t-PEPSI sequence is less sensitive than a conventional GRE sequence, we recommend it in patients with severe TBI, especially if they are uncooperative or medically unstable.

References

1. McLellan DR. **The structural bases of coma and recovery: insights from brain injury in humans and experimental animals.** In: Sandel ME, Ellis DW, eds. *The Coma-Emerging Patient.* Philadelphia: Hanley & Belfus; 1990:389–407
2. Graham DI. **Neuropathology of head injury.** In: Narayan RK, Wilburger JE, Povlishock JT, eds. *Neurotrauma.* New York: McGraw-Hill; 1996:43–59
3. Meythaler JM, Peduzz JD, Eleftheriou E, Novack TA. **Current concepts: diffuse axonal injury-associated traumatic brain injury.** *Arch Phys Med Rehabil* 2001;82:1461–1471
4. Gentry LR. **Imaging of closed head trauma.** *Radiology* 1994; 297:1–17
5. Wardlaw JM, Statham PFX. **How often is haemosiderin not visible on routine MR following traumatic intracerebral haemorrhage?** *Neuroradiology* 2000;42:81–84
6. Scheid R, Preul C, Gruber O, Wiggins C, von Cramon Y. **Diffuse axonal injury associated with chronic traumatic brain injury: evidence from T2*-weighted gradient-echo imaging at 3T.** *AJNR Am J Neuroradiol* 2003;24:1049–1056
7. Mittl RL, Grossman RI, Hiehle JF, et al. **Prevalence of MR evidence of diffuse axonal injury in patients with mild head injury and normal head CT findings.** *AJNR Am J Neuroradiol* 1994;15(8):1583–1589
8. Adams JH, Doyle D, Ford I, Gennarelli TA, Graham DI, McLellan DR. **Diffuse axonal injury: definition, diagnosis and grading.** *Histopathology* 1989;15:49–59
9. Parizel PM, Ozsarlak O, Van Goethem JW, et al. **Imaging findings in diffuse axonal injury after closed head trauma.** *Eur Radiol* 1998;8:960–965
10. Bradley WG. **MR appearance of hemorrhage in the brain.** *Radiology* 1993;189:15–26
11. Patel MR, Edelman RR, Warach S. **Detection of hyperacute primary intraparenchymal haemorrhage by magnetic resonance imaging.** *Stroke* 1996;27:2321–2324
12. Tong KA, Ashwal S, Holshouser BA, et al. **Hemorrhagic shearing lesions in children and adolescents with posttraumatic diffuse axonal injury: improved detection and initial results.** *Radiology* 2003;227:332–339
13. Fazekas F, Kleinert R, Roob G, et al. **Histopathologic analysis of foci of signal loss on gradient-echo T2*-weighted MR images in patients with spontaneous intracerebral hemorrhage: evidence of microangiopathy-related microbleeds.** *AJNR Am J Neuroradiol* 1999;20:637–642
14. Kuzma BB, Goodman JM. **Improved identification of axonal shear injuries with gradient echo MR technique.** *Surg Neurol* 2000;53:400–402
15. Yanagawa Y, Tsushima Y, Tokumaru A, et al. **A quantitative analysis of head injury using T2-weighted gradient-echo imaging.** *J Trauma* 2000;49:272–277
16. Edelman R, Wielopolski P, Schimitt F. **Echo-planar MR imaging.** *Radiology* 1994;192:600–612
17. Patel MR, Siewert B, Klufas R, Yousuf N, Edelman RR, Warach S. **Echoplanar MR imaging for ultra-fast detection of brain lesions.** *AJR Am J Roentgenol* 1999;173(2):479–485
18. Posse S, Dager SR, Richards TL, et al. **In vivo measurement of regional brain metabolic response to hyperventilation using magnetic resonance: proton echo planar spectroscopic imaging (PEPSI).** *Magn Reson Med* 1997;37:858–865
19. Posse S, Wiese S, Gembris D, et al. **Enhancement of BOLD-contrast sensitivity by single-shot multi-echo functional MR imaging.** *Magn Reson Med* 1999;42:87–97
20. Hagberg GE, Indovina I, Sanes JN, Posse S. **Real-time quantification of T2* changes using multiecho planar imaging and numerical methods.** *Magn Reson Med* 2002;48(5):877–882
21. Liang L, Korogi Y, Sugahara T, et al. **Detection of intracranial hemorrhage with susceptibility-weighted MR sequences.** *AJNR Am J Neuroradiol* 1999;20:1527–1534
22. Kinoshita T, Okudera T, Tamura H, Ogawa T, Hatazawa J. **Assessment of lacunar haemorrhage associated with hypertensive stroke by echo-planar gradient-echo T2*-weighted MRI.** *Stroke* 2000;31: 1646–1650
23. Lin Doris DM, Filippi CG, Steever AB, Zimmerman RD. **Detection of intracranial hemorrhage: comparison between gradient-echo images and b0 images obtained from diffusion-weighted echo-planar sequences.** *AJNR Am J Neuroradiol* 2001;22:1275–1281
24. Jennett B, Bond M. **Assessment of outcome after severe brain damage.** *Lancet* 1975;1:480–484
25. Teasdale TW, Jennett B. **Assessment of coma and impaired consciousness: a practical scale.** *Lancet* 1974;11:81–84
26. Smith DH, Chen XH, Pierce JE, et al. **Progressive atrophy and neuron death for one year following brain trauma in the rat.** *J Neurotrauma* 1997;14:715–727
27. Kampfl A, Schmutzhard E, Franz G, et al. **Prediction of recovery from post-traumatic vegetative state with cerebral magnetic resonance imaging.** *Lancet* 1998;351:1763–1767
28. Raghupathi R, Graham DI, McIntosh TK. **Apoptosis after traumatic brain injury.** *J Neurotrauma* 2000;17:927–938
29. Garnett MR, Cadoux-Hudson TA, Styles P. **How useful is magnetic resonance imaging in predicting severity and outcome in traumatic brain injury?** *Curr Opin Neurol* 2001;14(6):753–757
30. Adams JH, Graham DI, Gennarelli TA, Maxwell WL. **Diffuse axonal injury in non missile head injury.** *J Neurol Neurosurg Psychiatry* 1991;54:481–483
31. Gean AD. *Imaging of Head Trauma.* New York: Raven; 1994: 207–248
32. Smith DH, Nonaka M, Miller R, et al. **Immediate coma following inertial brain injury dependent on axonal damage in the brainstem.** *J Neurosurg* 2000;93:315–322
33. Toide K. **Effects amantadine on dopaminergic neurons in discrete regions of the rat brain.** *Pharm Res* 1990;7:670–667
34. Meythaler JM, Brunner RC, Johnson A, Novack TA. **Amantadine to improve neurorecovery in traumatic brain injury-associated diffuse axonal injury: a pilot double-blind randomized trial.** *J Head Trauma Rehabil* 2002;17:300–313
35. Goldstein LB. **Pharmacologic modulation of recovery after stroke: clinical data.** *J Neurol Rehabil* 1991;5:129–140
36. Matsuda W, Matsumura A, Komatsu Y, Yanaka K, Nose T. **Awakenings from persistent vegetative state: report of three cases with parkinsonism and brain stem lesions on MRI.** *J Neurol Neurosurg Psychiatry* 2003;74:1571–1573
37. De La Paz RL. **Echo-planar Imaging.** *Radiographics* 1994;14: 1045–1048
38. Wolansky LJ, Sheth MP, Axen R, Prased V. **Double-shot magnetic resonance imaging of cerebral lesions: fast spin-echo versus echo planar sequences.** *J Neuroimaging* 2000;10:131–137
39. Reichenbach JR, Essig M, Haacke EM, et al. **High-resolution venography of the brain using magnetic resonance imaging.** *Magn Reson Materials Biol Phys Med* 1998;6:62–69

40. Lee BCP, Vo KD, Kido DK, et al. **MR high-resolution blood oxygenation level-dependent venography of occult (low-flow) vascular lesions.** *AJNR Am J Neuroradiol* 1999;20:1239–1242
41. Besenski N. **Traumatic injuries: imaging of head injuries.** *Eur Radiol* 2002;12:1237–1252
42. Kampfl A, Franz G, Aichner FE, et al. **The persistent vegetative state after closed head injury: clinical and magnetic resonance imaging findings in 42 patients.** *J Neurosurg* 1998;88:809–816
43. Takaoka M, Tabuse H, Kumura E, et al. **Semiquantitative analysis of corpus callosum injury using magnetic resonance imaging indicates clinical severity in patients with diffuse axonal injury.** *J Neurol Neurosurg Psychiatry* 2002;73:289–293